

Simulation of CO₂ and H₂S Removal Using Methanol in Hollow Fiber Membrane Gas Absorber (HFPGA)

Majid Mahdavian¹, Hossein Atashi^{1*}, Morteza Zivdar¹, Mahmood Mousavi²

¹Department of Chemical Engineering, University of Sistan and Baluchestan, Zahedan, Iran

²Department of Chemical Engineering, Ferdowsi University of Mashhad, Mashhad, Iran

Email: *h.ateshi@hamoon.usb.ac.ir, majid_mahdavian@yahoo.com

Received September 1, 2011; revised October 25, 2011; accepted November 10, 2011

ABSTRACT

Application of methanol solvent for physical absorption of CO₂ and H₂S from CO₂/H₂S/CH₄ mixture in gas-liquid hollow fiber membrane gas absorber (HFPGA) was investigated. A computational mass transfer (CMT) model for simulation of HFPGA in the case of simultaneous separation of CO₂ and H₂S was developed. The membrane gas absorber model explicitly calculates for the rates of mass transfer through the membrane and components concentration profiles. Due to the lack of experimental data in the literature, the model was validated using available individual components' water absorption data. The numerical predictions were in good agreement with the experimental data. The effects of operating conditions such as liquid velocity, gas velocity, temperature and pressure were analyzed. It is shown that methanol solvent can successfully be used for CO₂ and H₂S removal in membrane gas absorber. Also it is found that the concentration distribution of CO₂ and H₂S in the gas phase along the fiber length obeys plug flow model whereas in the methanol absorbent deeply affected by the interface concentration, absorbent velocity and diffusivity. In addition, it is shown that application of membrane gas absorber using methanol absorbents for H₂S removal and at higher flow rate is more efficient. Moreover, at operating pressures above 10 atm even at low absorbent rate, H₂S concentration depletion is relatively complete while at 1 atm this value is about 30%. This means that removal efficiency decreases with an increase in temperature and it is more important especially for H₂S.

Keywords: Computational Mass Transfer (CMT); Membrane Gas Absorber; CO₂ and H₂S Separation; Physical Absorption; Methanol

1. Introduction

Some industrial gas streams (such as natural gas processing, petroleum refineries, petrochemicals) frequently contain H₂S and CO₂ as impurities. All of these gases requires treatment before delivery to the pipeline. It is reported that CO₂ is representing about 80% of greenhouse gases and half of the CO₂ emissions are produced by industrial plants such as fossil-fuel-fired power plants, iron, steel and cement works [1]. Also carbon dioxide is a common contaminant of natural gas and must be removed to a level of <8% (usually <2%) to minimize corrosion of the pipeline. Hydrogen sulfide removal is also desirable to reduce corrosion. In many cases it is necessary from the health and safety standpoint [2].

The most well known technology for recovery/removal of CO₂ and H₂S is solvent absorption. This technology was established over 80 years ago in the chemical and oil industrials for the removal of acid gases from natural gas streams. For the removal of CO₂ and H₂S, traditiona-

lly absorption processes like packed and plate columns are utilized [3]. Because these generally require large space and high investment cost, the emphasis of designing most of these operations is towards maximizing the mass transfer rate by creating as much interfacial area as possible [4]. In addition, they also suffer from several limitations including flooding, loading entrainment, foaming, weeping, etc. In recent years, the demand for alternative technologies has increased and many researchers have looked for new technologies to enhance the efficiency of absorption processes. Membrane-based absorption technique has been introduced as an emerging technology for the recovery/removal of gases (like CO₂, H₂S, SO₂, NH₃, VOC, etc.) from various industrial process gas streams [5]. In addition to gas/liquid, this technology also has found applications in numerous liquid/liquid applications such as fermentation, pharmaceuticals, wastewater treatment, semiconductor manufacturing, carbonation of beverages, metal ion extraction, protein extraction, osmotic distillation and other operations [6].

Membrane gas absorbers are devices that achieve two-

*Corresponding author.

phase mass transfer through diffusion without dispersing one phase within another. Such a device employs a porous membrane acts as a non-selective barrier between both phases where the gas and the absorbent solution flow on two sides of a membrane [5]. The membranes are usually microporous and can be both hydrophobic and hydrophilic. Hydrophobic microporous membranes like polypropylene (PP), polytetrafluoroethylene (PTFE) and polyvinylidene fluoride (PVDF) membranes have received increasing attention in recent years for using in membrane gas absorbers because of their good hydrophobicity [7]. These membrane absorber systems, generally in the form of hollow fibers with diameters of 0.5 mm - 1 mm in densely packed membrane modules, provide a high interfacial area ($500 \text{ m}^2/\text{m}^3$ - $2000 \text{ m}^2/\text{m}^3$) significantly greater than most traditional absorbers ($100 \text{ m}^2/\text{m}^3$ - $800 \text{ m}^2/\text{m}^3$) between two phases to achieve high overall rates of mass transfer. This significantly decreases the size required for the contactor [8]. Moreover, this kinds of contacting devices offers a number of important advantages over conventional dispersed phase contactor for gas sorption, such as large interfacial area between gas and liquid flow (up to two orders of magnitude more surface area per volume than conventional contactors), no flooding and foaming phenomena, independent control of gas and liquid flow rates, high efficiency, the possibility of combining absorption and desorption in one single compact module, energy intensive, and so on (as an example of review, see Gabelman *et al.* [5]).

Chemical absorbents like amines and amino acid salts are extensively used in the removal of impurities from gas mixtures. Physical absorbents have been of considerable interest in the development of gas treatment solvents, especially when the partial pressure of undesirable impurity is high. Some of the physical solvents used commercially are propylene carbonate (PC), *n*-formyl morpholine (NFM), dimethyl ethers of polyethylene glycol (DEPG), and *n*-methyl-pyrrolidone (NMP) (see more example in [9]). Physical solvents can be a possible alternative to chemical solvents in certain areas of applications, although they are less effective than chemical absorbents (*i.e.* the specific absorption rate into physical absorbents in comparison with chemical solvents is less). But they can be regenerated by just pressure reduction method without large amount of heat supply and thus excessive energy savings can be obtained [9]. An economical analysis must be done to select the best choice of solvent. In addition, they can be used as pre-treatment solvent in the development of hybrid systems. The most well known physical absorbent is water. However, its economics are limited by the relatively low solubility which leads to larger amounts of circulation rate, *i.e.* the higher investment costs as well as the higher operating costs [10]. However, there are good organic solvents which

possess a much higher solvent capacity than water. Among the physical solvents, *n*-methyl-2-pyrrolidone (NMP), methanol and propylene carbonate (PC) are popular as gas treating solvents. Methanol has a high thermal and chemical stability, low vapor pressure, and is not corrosive. It is able to absorb acid gases, hydrocarbons, mercaptans and water. Moreover, it is produced in big quantity and readily available [10]. This properties make it highly effective for processing a wide range of compositions.

The applications of hollow fiber gas-liquid membrane gas absorber for acid gas removal specially carbon dioxide from gas mixtures have been studied by several researchers. In this case, a large number of experimental absorption studies and theoretical modeling analyses have been performed with physical or chemical absorbent liquids such as pure water, aqueous amine solution, aqueous sodium hydroxide solution, aqueous potassium carbonate solution, aqueous blended solvents, etc. [11-14]. Some authors have explored possible simultaneous removal of H_2S and CO_2 in hollow fiber membrane gas absorber using MEA [1] and DEA [15]. However, of the authors considering chemical absorption, few have worked with physical solvents as would be the good choice in membrane gas absorber process. There have been few attempts to address possible physical absorption in hollow fiber membrane gas absorbers [16-18] that mostly describes the water performance and theoretical analysis of simultaneous removal of CO_2 and H_2S using methanol absorbent in HFMGA has not been discussed by researchers.

In the present work, after modification of 2D mathematical model, this new process has been applied for CO_2 and H_2S capture from carbon dioxide/hydrogen sulfide/methane mixture (when the partial pressures of CO_2 and H_2S are 10% of total pressure) using methanol (as an example of physical absorbent) absorbent and its potential possibility for carbon dioxide and hydrogen sulfide removal has been evaluated. It should be mentioned that areas of possible HFMGA process for gas treatment using physical solvent with economic considerations will be reported in another work. This work was performed using CFD tool with respect to solubility behavior. CFD has been largely used as a powerful tool to model membrane separation processes. It is able to simulate the concentration, temperature and velocity fields as well as the transport parameters and operating efficiency.

2. Model Development

In this paper, a steady-state two-dimensional mathematical model has been modified (e.g. [1,12]) to describe the physical absorption of carbon dioxide and hydrogen sulfide in the polymeric hollow fiber membrane gas absorber (using methanol absorbent as the absorption liquid).

The model describes the mass transfer in the gas, membrane and liquid phases. Axial and radial diffusion inside the shell, through the membrane, and within the tube side of the membrane gas absorber have been considered in the model equations. It allows studying the effect of membrane wetting on the mass transfer through the membrane and also the effect of operating conditions (gas and liquid flow rates, temperature), solvent affinity (H) and flow pattern (counter current or co current arrangement) on the carbon dioxide and hydrogen sulfide removal efficiencies.

This model assumes that the fibers are distributed evenly through the shell space, which allows the results obtained with a single fiber to be generalized to the entire module. Model results are based on “non-wetted mode” in which the gas mixture filled the membrane pores.

The following assumptions are made to develop the governing mass transfer differential equations: 1) fully developed parabolic velocity profile in the hollow fiber under laminar flow conditions; 2) the mixture gases flow inside the shell are ideal gas; 3) Happel’s free surface model [19] is used to characterize the velocity profile at the shell side; 4) the physical properties of the fluid are constant; 5) the Henry’s law is applicable for gas-liquid interface; 6) no absorption of bulk and inert gases; 7) pitch and placing of the fibers are uniform; 8) no pore blockage.

2.1. Transport Model for the Hollow Fiber Membrane Gas Absorber

In order to describe the mass transfer and develop the equations of mathematical model in the hollow fiber membrane gas absorber, a material balance has been applied for a segment of a hollow fiber, as shown in **Figure 1** in the shell, membrane and tube sides. Also, the computational domain used for the numerical simulation is shown in **Figure 1**. This model is based on the idea that two concentric cylinders are used as the model for fluid flowing out of the fibers and so only portion of fluid surrounding the fiber is considered and may be approximated as circular cross section [19]. The fluid flow is described using the fully developed laminar flow model in the tube side, whereas the fluid flow in the shell side is characterized by the Happel’s free surface model.

The position $r = 0$ is the center of the fiber and r_1 , r_2 and r_3 are the inner, outer and Happel’s free model radii of the fiber, respectively (**Figure 1**). The radius of Happel’s free surface model is calculated to be $r_3 = 720 \mu\text{m}$. Dimensions of the hollow-fiber membrane gas absorber are listed in **Table 1**. The gas mixture consists of carbon dioxide, hydrogen sulfide and methane is fed to the shell side at $z = L$, while the liquid (methanol) is passed through the tube side at $z = 0$. Carbon dioxide and hydrogen sulfide are removed from the mixture by diffusing

through the membrane due to a concentration gradient and then absorbing with the solvent.

2.1.1. Equations Describing the Shell Side

Convective-diffusion equation for the component i using Fick’s law of diffusion, when chemical reaction is taking place, can be written as:

$$\partial C_{i,\text{shell}} / \partial t + \nabla \cdot (-D_{i,\text{shell}} \nabla C_{i,\text{shell}} - C_{i,\text{shell}} V_{i,\text{shell}}) = R_{i,\text{shell}} \quad (1)$$

where C_i , $D_{i,\text{shell}}$, R_i and V_{shell} denote the local concentration of the component i , the diffusivity of the component i , reaction rate of the component i and axial velocity in shell side, respectively. According to the Happel’s free surface model [19], the velocity profile in the shell side may be obtained. For this purpose, a momentum balance over a thin cylindrical shell is integrated twice to obtaining the following equation for the shell side velocity distribution, which have been applied by several authors (e.g. [20,21]):

$$V_{\text{shell}} = 2V_{\text{ave-shell}} \left(1 - \left(\frac{r_2}{r_3} \right)^2 \right) \cdot \left(\frac{(r/r_3)^2 - (r_2/r_3)^2 + 2 \ln(r_2/r)}{3 + (r_2/r_3)^4 - 4(r_2/r_3)^2 + 4 \ln(r_2/r_3)} \right) \quad (2)$$

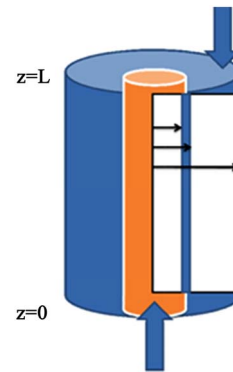


Figure 1. The schematic diagram of a hollow fiber membrane and computational domain.

Table 1. Specifications of the membrane gas absorber.

| Parameter | Value |
|-------------------|-----------------------|
| Module I.D. (m) | 4.35×10^{-3} |
| Module O.D. (m) | 6.35×10^{-3} |
| Fiber O.D. (m) | 9.07×10^{-4} |
| Fiber I.D. (m) | 6.07×10^{-4} |
| Module length (m) | 0.3 |
| Fiber length (m) | 0.2725 |
| No. of fibers | 9 |

where V_{shell} is the velocity component inside the shell, $V_{ave-shell}$ is the shell average velocity in the axial direction, r_2 (m) is the outer fiber radius and r_3 (m) is Hapel's free surface model radius defined as:

$$r_3 = r_2 \sqrt{1/(1-\phi)} \quad (3)$$

Packing density (ϕ) can be defined as the ratio of total surface area of membrane to the cross-sectional area of the module and ϕ is calculated as:

$$\phi = n \left(\frac{r_2}{r_4} \right)^2 \quad (4)$$

where n is the number of fibers and r_4 is the inner radius of the MGA. The partial differential equation of the steady state mass balance for cylindrical coordinates, where no reaction takes place in the shell side is obtained and it is given as follows:

$$D_{i-shell} \left(\frac{\partial^2 C_{i-shell}}{\partial r^2} + \frac{1}{r} \frac{\partial C_{i-shell}}{\partial r} + \frac{\partial^2 C_{i-shell}}{\partial z^2} \right) = V_{shell} \frac{\partial C_{i-shell}}{\partial z} \quad (5)$$

The boundary conditions are the following ($i = CO_2, H_2S$)

$$\text{At } z = L : C_{i-shell} = C_{0,i-shell} \quad (6)$$

$$\text{At } r = r_2 : C_{i-shell} = C_{i-mem} \quad (7)$$

$$\text{At } r = r_3 : \partial C_{i-shell} / \partial r = 0 \text{ (symmetry)} \quad (8)$$

2.1.2. Equations Describing the Membrane Side

Mass transfer takes place through the membrane pores without mixing between phases and the transfer equation inside the pores can be derived without considering convection. The membrane diffusivity of species within the pores should be employed instead of the ordinary diffusivity. This parameter can be defined as $D_{i-mem} = D_i \varepsilon / \tau$. The steady state material balance for the transport of diffusing components ($i = CO_2, H_2S$) inside the membrane can be considered for non-wetting condition, where pores filled by the gas phase. For the non-wetting case, no chemical reactions will be considered in the membrane.

$$D_{i-mem} \left(\frac{\partial^2 C_{i-mem}}{\partial r^2} + \frac{1}{r} \frac{\partial C_{i-mem}}{\partial r} + \frac{\partial^2 C_{i-mem}}{\partial z^2} \right) = 0 \quad (9)$$

$$\text{At } r = r_1 : C_{i-mem} = C_{i-tube} / m_i \quad (10)$$

$$\text{At } r = r_2 : C_{i-mem} = C_{i-shell} \quad (11)$$

In the partial wetted mode, additional equations are required to describe diffusion-reaction inside the wetted parts of the pores. In this case the pores are both gas and liquid-filled (wetted and non-wetted parts) and the transport of the species i generally depends on its diffusion coefficient into the liquid [22].

2.1.2.1. Non-Wetted Part of the Membrane

$$D_{i-drymem} \left(\frac{\partial^2 C_{i-drymem}}{\partial r^2} + \frac{1}{r} \frac{\partial C_{i-drymem}}{\partial r} + \frac{\partial^2 C_{i-drymem}}{\partial z^2} \right) = 0 \quad (12)$$

Boundary conditions are:

$$\text{At } r = r_2 : C_{i-drymem} = C_{i-shell} \quad (13)$$

$$\text{At } r = r_w : C_{i-drymem} = C_{i-wetmem} / m_i \quad (14)$$

2.1.2.2. Wetted Part of the Membrane

$$D_{i-wetmem} \left(\frac{\partial^2 C_{i-wetmem}}{\partial r^2} + \frac{1}{r} \frac{\partial C_{i-wetmem}}{\partial r} + \frac{\partial^2 C_{i-wetmem}}{\partial z^2} \right) + \varepsilon R_i = 0 \quad (15)$$

Boundary conditions are:

$$\text{At } r = r_w : C_{i-wetmem} = m_i C_{i-drymem} \quad (16)$$

$$\text{At } r = r_1 : C_{i-wetmem} = C_{i-tube}, C_{\text{solvent-tube}} = C_{\text{solvent-mem}} \quad (17)$$

where m is dimensionless distribution coefficient.

2.1.3. Equations Describing the Tube Side

The partial differential equation of the steady state mass balance for each species during simultaneous mass transfer in a non-reactive absorption system is obtained and can be expressed as:

$$D_{i-tube} \left(\frac{\partial^2 C_{i-tube}}{\partial r^2} + \frac{1}{r} \frac{\partial C_{i-tube}}{\partial r} + \frac{\partial^2 C_{i-tube}}{\partial z^2} \right) = V_{tube} \frac{\partial C_{i-tube}}{\partial z} \quad (18)$$

The left-hand side of the above equation represents the diffusion and reaction terms, whereas the right-hand side is the convection term. Considering laminar flow, Navier-Stokes equations and the equation of continuity can be solved for fluid flow in a cylindrical pipe, therefore velocity distribution in the tube in the z direction can then be obtained as [22]:

$$V_{tube} = 2V_{ave-tube} \left(1 - \left(\frac{r}{r_1} \right)^2 \right) \quad (19)$$

where V , r and r_1 are the average velocity in the lumen, the radial distance and the radius of the lumen, respectively. The following boundary conditions are considered:

$$\text{At } z = 0 : C_{\text{solvent-shell}} = C_{0,\text{solvent-tube}} \quad (20)$$

$$\text{At } r = 0 : \partial C_{i-tube} / \partial r = 0 \text{ (symmetry)} \quad (21)$$

$$\text{At } r = r_1 : C_{i-tube} = m_i C_{i-mem} \quad (22)$$

2.2. Physical Properties and Numerical Solution

Simulation of membrane gas absorber requires data on

physicochemical properties used as input parameters in the model such as solubility and diffusivity of the relevant components in each phase. The distribution coefficient of CO_2 was taken from Versteeg *et al.* [23] and distribution coefficient of H_2S was taken from Carroll *et al.* [24] as a function of temperature in water. Henry's constant of CO_2 and H_2S for methanol as a function of temperature was reported by Lunsford *et al.* [25]. Liquid-phase diffusivities of CO_2 [23] and H_2S [26] in water were estimated by the equations proposed by Versteeg and Cussler respectively and their value in methanol were estimated using the correlation given by Diaz *et al.* [27]. Gas-phase diffusivities of CO_2 and H_2S were estimated using the correlation given by Diaz *et al.* [27] and Cussler *et al.* [26]. Gas-filled membrane phase diffusivities were corrected for membrane porosity and tortuosity. The values for other data were obtained from [28,29].

In order to solve the coupled partial differential equations for the tube, membrane and shell sides with the appropriate boundary conditions and physical and chemical properties for CO_2 and H_2S , FEMLAB software has been used.

3. Results and Discussion

3.1. Model Validation

The model of simultaneous absorption of CO_2 and H_2S using methanol in hollow fiber membrane gas absorber was validated using available individual components' absorption data of Al-Marzouqi *et al.* [20] and Faiz *et al.* [30] for physical absorption of CO_2 and H_2S in water, respectively, since we didn't find any reported experimental data for the type of the present work in the literature.

Comparison of the experimental data and the simulated results are shown in **Figures 2** and **3**. It should be noted that the type of hollow fiber MGA modules and the operating conditions applied for obtaining the mentioned experimental data differ significantly with each other and we applied the exact conditions for each case. Results of both validations for physical absorption of CO_2 and H_2S are shown in **Figures 2** and **3**, respectively. **Figure 2** shows the calculation of the model with the experimental results of percent CO_2 removal as a function of water flow rate at the gas flow rate of 200 ml/min and **Figure 3** shows the percent H_2S removal and the outlet H_2S concentration as a function of inlet concentration of H_2S in the gas phase at gas velocity of 5.1 m/s and liquid velocity of 0.092 m/s. Clearly the model predictions are in good agreement with the two set of CO_2 and H_2S absorption data and it shows that the numerical model accurately predicts the experimental data for both gases.

3.2. Concentration Distribution of CO_2 and H_2S

A steady state component concentration distribution is

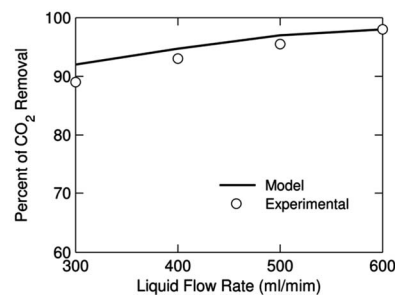


Figure 2. Comparison between experimental [20] and simulated CO_2 removal efficiency.

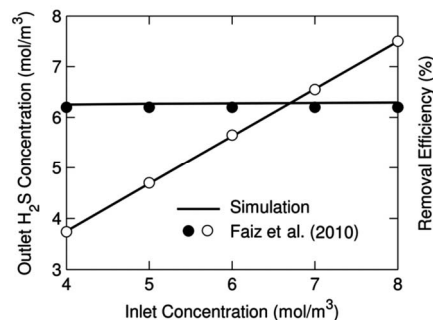


Figure 3. Comparison between model data [30] and simulated H_2S gas outlet concentration and removal efficiency.

established inside the shell, membrane, and within the tube side of the hollow fiber membrane gas absorber that affects mass transfer coefficient, removal efficiency and mass transport. Numerically calculated carbon dioxide and hydrogen sulfide concentration distribution in each of the three phases are depicted in **Figures 4** and **5**, respectively. In order to compare the difference between concentration profiles of CO_2 and H_2S effectively, equal input concentration in gas phase is applied. The solubility of CO_2 and H_2S in methanol is linearly proportional to their partial pressure in the gas mixture and, hence, it can be modeled according to Henry's law. As expected, it can be seen that the concentration near the membrane-liquid wall significantly affected by the interface concentration, whereas the CO_2 and H_2S concentrations on the shell side slightly decrease in the radial direction. The concentration profile is discontinuous at the gas filled membrane-liquid interface based on the equilibrium relationship.

Due to the dimensions of the hollow fiber, the computational domain is the area of membrane length multiplied by Happel's free surface model width. It is important to note that since the fiber is 900 times longer than its radial dimension (in this case, 0.3 mm in radius and 27 cm in length), a scaling factor of 90 has been applied in the z direction in order to reduce computational cost.

It is worth mentioning that the sensitivity grid-dependence analysis of the method of solution to the mesh size was performed in order to ensure that the numerical solution is not affected by the specification of the mesh size.

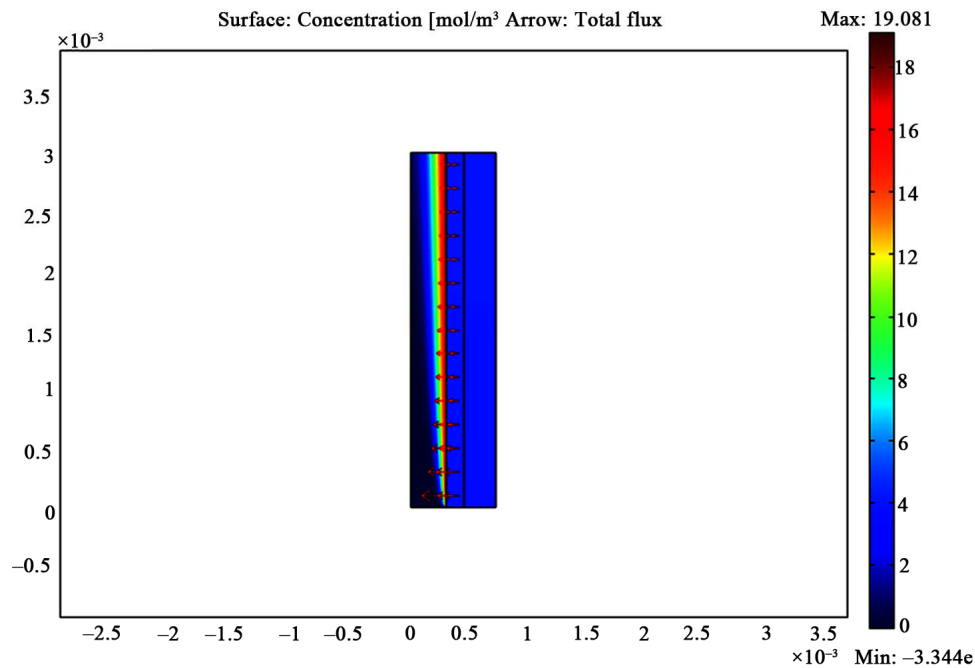


Figure 4. CO₂ concentration distribution in computational domain for $V_L = 0.1$ m/s, $V_G = 3$ m/s and $T = 298$ K.

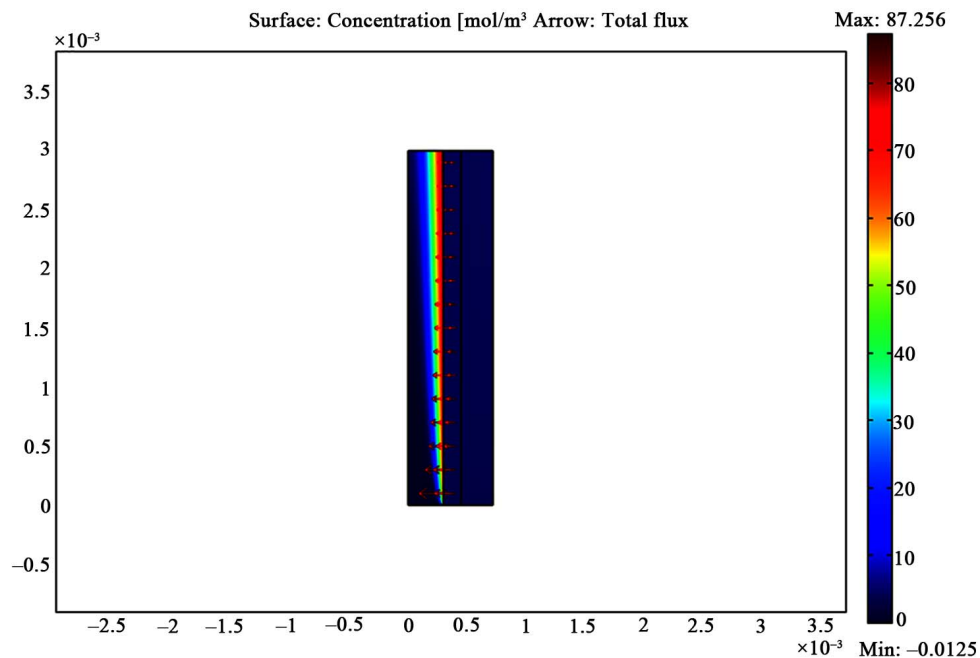


Figure 5. H₂S concentration distribution in computational domain for $V_L = 0.1$ m/s, $V_G = 3$ m/s and $T = 298$ K.

The importance of a fine mesh adjacent to the membrane wall is obvious from the components concentration distribution shown in **Figures 4** and **5**.

Figures 6 and **7** show the numerically calculated dimensionless radial concentration profile of CO₂ and H₂S as a function of dimensionless length at different cross sections along fiber length, *i.e.* $z/L = 0.1, 0.5, 0.9$ (**Figure 6**) and at two different absorbent velocities (**Figure 7**).

With respect to these figures, there is a concentration drop close to the absorbent-membrane interface at the membrane wall in the methanol absorbent phase for both gases. Concentration depletion for CO₂ and H₂S in liquid phase has the same trend but there is a sharper reduction in H₂S concentration in comparison with CO₂ concentration which is attributed to higher solubility of H₂S in the methanol absorbent.

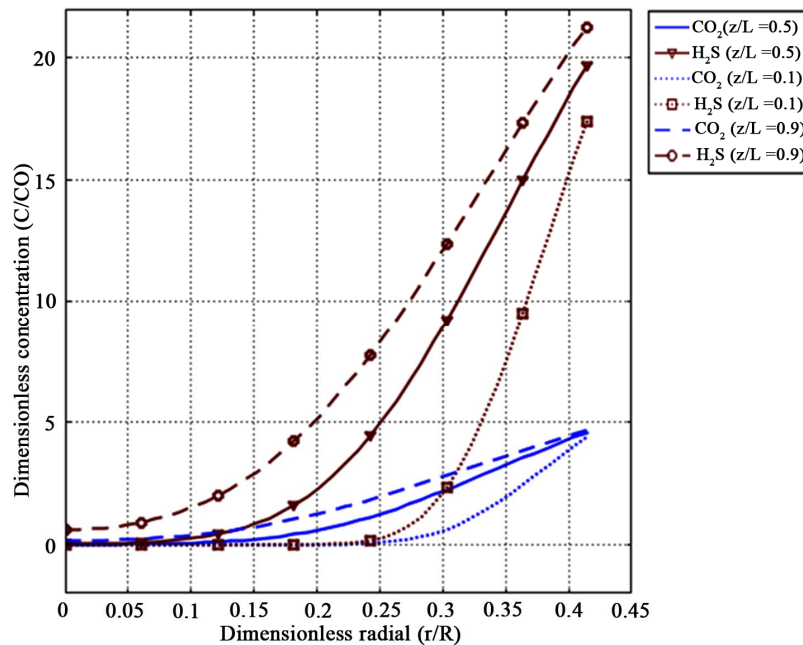


Figure 6. CO₂ and H₂S radial tube side concentration profiles along fiber length for $z/L = 0.1, 0.5, 0.9, V_L = 0.1 \text{ m/s}, V_G = 3 \text{ m/s}$ and $T = 298 \text{ K}$.

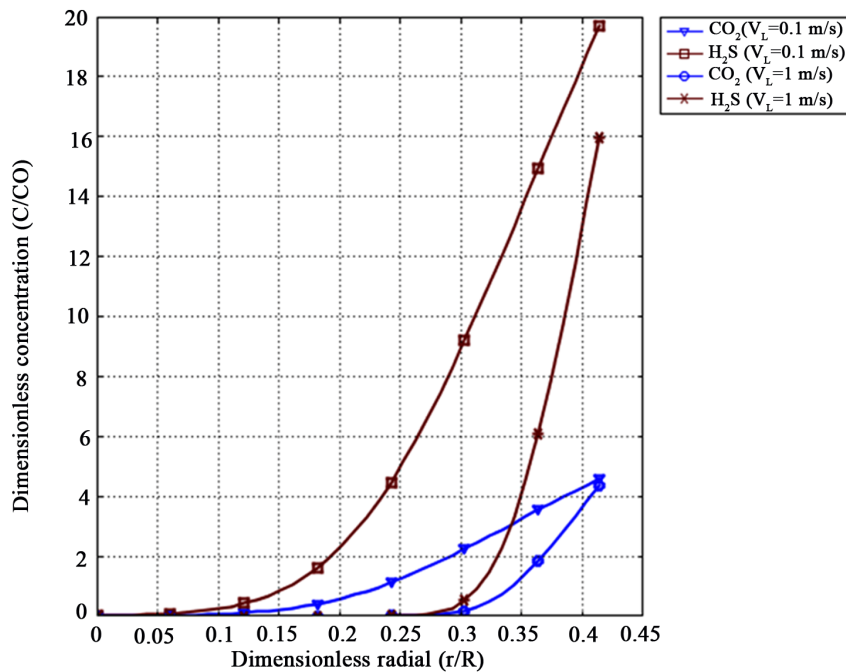


Figure 7. Effect of absorbent velocity on CO₂ and H₂S radial tube side concentration profiles for $V_G = 3 \text{ m/s}, z/L = 0.5$ and $T = 298 \text{ K}$.

The results indicate that penetration depth increases with distance from methanol absorbent entrance ($z/L = 0$) and, therefore, components diffuse into liquid phase from membrane interface. Note that since liquid phase is very thin, it acts as film layer. With respect to the components diffusivities, liquid velocity and dimension of fiber, it is seen that the contact time is not enough that diffusion

entirely affects the liquid phase and absorbed species do not distribute rapidly in radial direction before absorbent leaves the fiber (dimensionless Gz number conception). However, at higher inlet liquid velocity, the depletion of component concentration is faster. The reason is that the axial convective flow decreases with radial diffusion.

Figure 8 shows the axial CO₂ and H₂S concentration

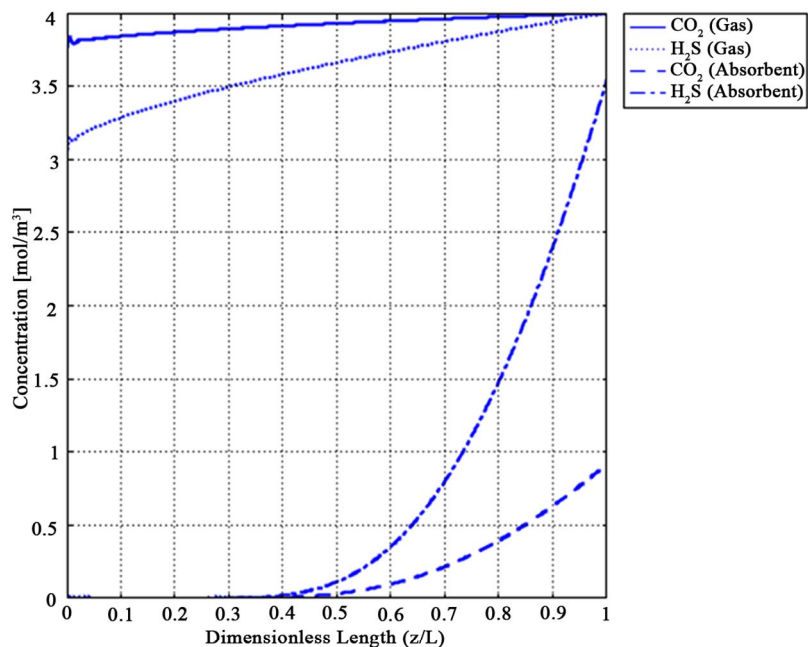


Figure 8. CO₂ and H₂S concentration profile in the axial direction in both shell and tube sides for $V_L = 0.1$ m/s, $V_G = 3$ m/s, $C_{0,CO_2} = C_{0,H_2S} = 4$ mol/m³ and $T = 298$ K.

profiles in absorbent and gas phase. For absorbent phase, tube center line ($r = 0$) and for gas phase Happel's radius ($r = r_3$) is selected. It can be seen that in the case of methanol absorbent, the CO₂ concentration depletion in the gas and amount of absorbed are low in comparison with the H₂S. It obviously indicates the higher capacity of methanol in absorption of H₂S. Based on the bulk concentration of CO₂ and H₂S, removal efficiencies are about 12.9% and 29.3% throughout the fiber, respectively. Moreover, in 50% and 40% of the fiber length, the concentrations are still zero for CO₂ and H₂S, respectively.

3.3. Effect of Absorbent and Gas Velocity on CO₂ and H₂S Removal Efficiencies

Figures 9 and 10 indicate the effect of absorbent and gas velocity on the removal efficiencies of CO₂ and H₂S using methanol absorbent in comparison with water absorbent. Wide range of velocities was selected for both absorbent and gas in order to provide a chance to gain a real insight into this effect. Considering these figures, CO₂ and H₂S removal efficiencies at given conditions increase with the increase in absorbent velocity. This effect is due to the increasing in driving force with entering fresh absorbent. Therefore, CO₂ and H₂S concentrations in gas phase reduce and removal efficiencies improved because of higher absorption rate. This effect is reported by several authors [1,30,31] for water absorbent in the case of physical absorbent in hollow fiber membrane gas absorber devices.

The results show that with increasing the liquid velocity,

the overall mass transfer coefficient increases. The reason is that in the case of physical absorption in membrane gas absorber, the controlling resistance for the mass transfer usually is liquid phase. The CO₂ and H₂S removal ability of methanol is illustrated in Figure 9 where the results are plotted for methanol in comparison with water absorbent. For example at the absorbent velocity of 3 m/s, the removal efficiencies using methanol absorbent are 34.7% and 84.3% and removal efficiencies using water absorbent are 13.8% and 21.6% for CO₂ and H₂S, respectively.

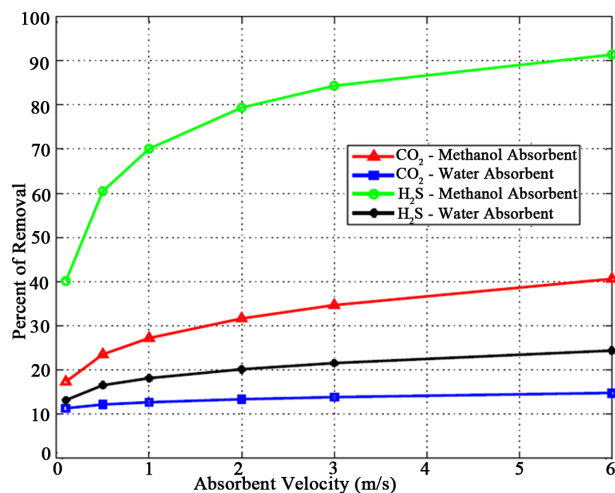


Figure 9. Effect of absorbent velocity on CO₂ and H₂S removal efficiencies for methanol and water absorbent at $V_G = 2$ m/s, $C_{0,CO_2} = C_{0,H_2S} = 4$ mol/m³ and $T = 298$ K.

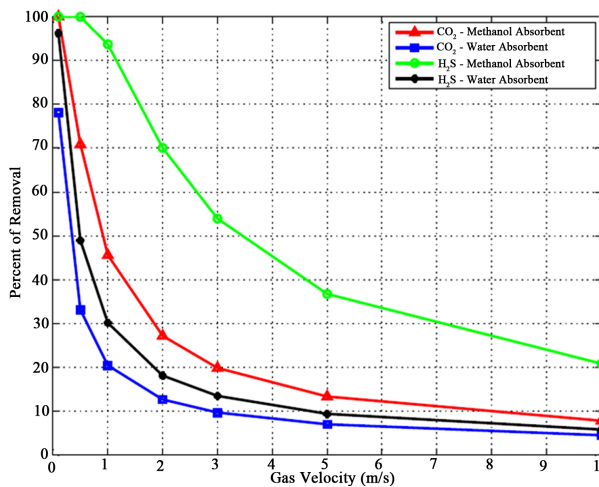


Figure 10. Effect of gas velocity on the CO₂ and H₂S removal efficiencies for methanol and water absorbent at $V_L = 1$ m/s, $C_{0,CO_2} = C_{0,H_2S} = 4$ mol/m³ and $T = 298$ K.

It is important to note that in the case of methanol (or water), the CO₂ removal efficiency reaches a relatively constant value whereas, H₂S removal efficiency increases by increasing the liquid velocity which leads to higher relative absorption rates in comparison with CO₂. This is due to the fact that for higher absorbent velocities due to the lower contact time, the absorbent liquid cannot reach saturation and maybe leaves the module unsaturated. In spite of reducing contact time at higher velocities, methanol absorbent (or water) leaves the module saturated with respect to its low CO₂ potential absorption whereas the H₂S potential absorption is high enough resulting in an unsaturated absorbent at the module exit. Relative absorption rate of CO₂ using methanol absorbent is in the range of 1.5 to 2.7 and relative absorption rate of H₂S using methanol absorbent is in the range of 2.9 to 3.75 in comparison with the case of water absorbent in this operating. Therefore, application of membrane gas absorber using methanol absorbent for H₂S removal and at higher flow rate is more efficient. In addition, methanol in comparison with other commercially available physical solvents has a lower viscosity, which increases mass transfer rates and decreases membrane area requirements and pressure drop over the fiber length. Note that in simultaneous absorption of CO₂ and H₂S using methanol in MGA when selective absorption of CO₂ and H₂S is desired, selectivity remains relatively constant with increasing the methanol absorbent flow rate.

Figure 10 shows the effect of gas velocity on the CO₂ and H₂S removal efficiencies for methanol absorbent at a given conditions in comparison with water absorbent. It can be seen that CO₂ and H₂S removal efficiencies decrease considerably with the increase in gas velocity. This effect is due to the fact that by increasing the gas velocity (or flow rate) the amount of input impurity (CO₂

and H₂S) increases at constant absorption ability and on the other hand, gas-liquid contact time decreases. As a result of these two negative effects, CO₂ removal efficiency decreases in the membrane gas absorber.

Note that reduction in removal efficiencies are not the same for equal velocity step size in both gas and absorbent due to the different gas-liquid contact time. For example, contact time decreases 67% when velocity changes from 1 m/s to 3 m/s while it decreases 40% when velocity changes from 3 m/s to 5 m/s.

3.4. The Effect of Temperature and Pressure on CO₂ and H₂S Removal Efficiency

Figure 11 shows gas phase CO₂ and H₂S concentration profiles in the axial direction at three different temperatures, *i.e.* 288 K, 298 K and 308 K. It can be seen that the outlet CO₂ and H₂S concentrations increase and the trend of concentration variations for CO₂ and H₂S are the same but for H₂S is more important: the higher the temperature, the higher the average component concentration in the gas phase and outlet stream (lower removal efficiency). The reason is a result of two opposite effects that as the temperature increases, the solubility of CO₂ and H₂S decrease and liquid-phase diffusion coefficients increase. In addition, temperature effects on CO₂ and H₂S concentration distribution in the radial direction are more important near the membrane-liquid interface in the liquid phase.

Generally, physical solvents are used for undesirable component removal from high-pressure gas streams. **Figure 12** shows the effect of pressure on CO₂ and H₂S removal efficiencies for methanol absorbent. In the case of application of membrane gas absorber at high pressures, methanol as a physical solvent is more efficient

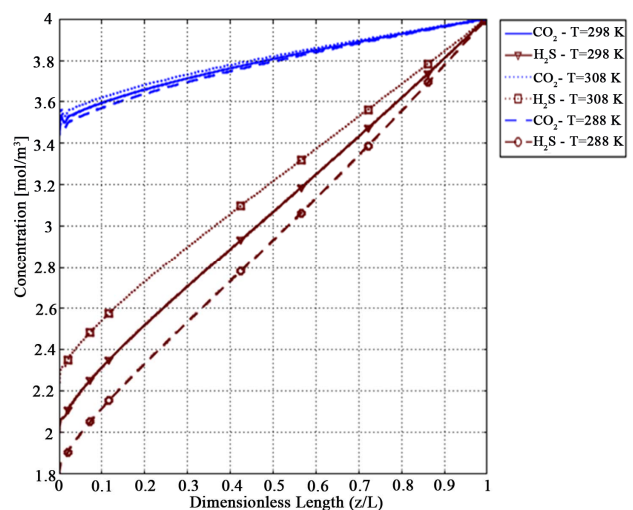


Figure 11. Effect of temperature on CO₂ and H₂S shell side concentration profile for $V_L = 1$ m/s, $V_G = 3$ m/s, $C_{0,CO_2} = C_{0,H_2S} = 4$ mol/m³ and $T = 298$ K.

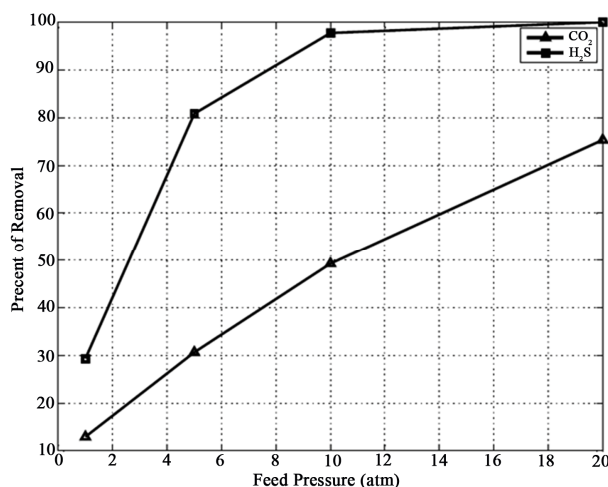


Figure 12. Effect of pressure on CO₂ and H₂S removal efficiencies for Methanol absorbent at $V_L = 0.1$ m/s, $V_G = 3$ m/s and $T = 298$ K.

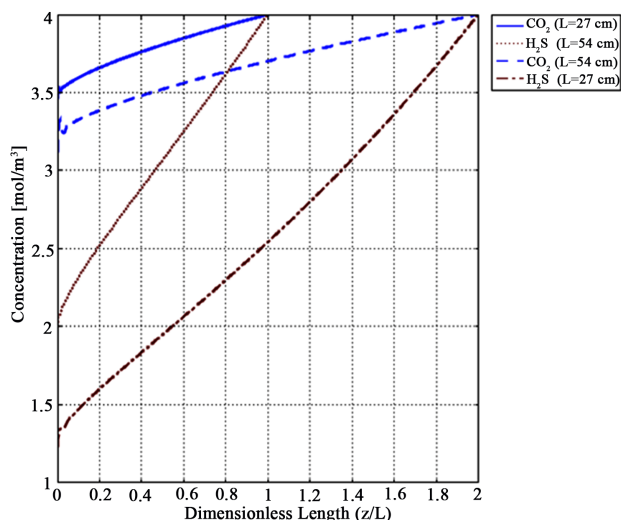


Figure 13. Effect of fiber length on CO₂ and H₂S concentration depletion in the gas phase along fiber length for methanol absorbent at $V_L = 1$ m/s, $V_G = 3$ m/s and $T = 298$ K.

and it might be an alternative to chemical solvents. At the module exit, complete H₂S concentration depletion is relatively above 10 atm while at 1 atm this value is about 30%. High partial pressure of CO₂ and H₂S or application of physical solvent with high absorption power leads to lower amounts of circulation. For example, the circulation rate need to absorption of CO₂ at a feed pressure of 10 atm in methanol is only about one-fourth of that circulation rate under 1 atm operating pressure.

Note that because the model results are based on “non-wetted mode” in which the gas mixture filled the membrane pores and assuming complete non-wetting conditions is valid at low pressure operations, it is expected that model overestimates CO₂ removal efficiency at high pressure. This can be attributed to mass transfer resistances

caused by partial wetting of pores in hollow fiber membrane [5].

The membrane length needed to achieve the desired removal efficiency is a significant parameter. By increasing the membrane length, the membrane area for mass transfer increased and thus, higher removal efficiency is achieved. As shown in **Figure 13**, we examined this effect for two membrane length, *i.e.* 27 cm and 54 cm. As a result of doubling the length, CO₂ removal efficiency increased by 60% and H₂S removal efficiency by 40% for $V_L = 1$ m/s, $V_G = 3$ m/s, $C_{0,CO_2} = C_{0,H_2S} = 4$ mol/m³ and $T = 298$ K.

4. Conclusions

The physical absorption of CO₂ and H₂S from CO₂/H₂S/CH₄ mixture (when the partial pressure of components is 10% of total pressure) was simulated. The effect of liquid velocity, gas velocity, temperature and pressure on removal efficiency was explored and the concentration distributions inside the shell, through the membrane, and within the tube side were studied. The results indicate that methanol has the potential as a low-cost, green physical solvent for CO₂ capture in HFMGA. Relative absorption rate of CO₂ using methanol absorbent is in the range 1.5 to 2.7 and relative absorption rate of H₂S using methanol absorbent is in the range 2.9 to 3.75 in comparison with the case of water absorbent for given operating conditions ($V_G = 2$ m/s, $C_{0,CO_2} = C_{0,H_2S} = 4$ mol/m³, $T = 298$ K). However, in simultaneously absorption of CO₂ and H₂S using methanol in MGA selectivity remains relatively constant with increasing the methanol absorbent flow rate. With increasing the temperature, the removal efficiencies slightly decreased. At high pressures, methanol as a physical solvent is more efficient and it might be an alternative to chemical solvents. Moreover, CO₂ removal efficiency about 60% and H₂S removal efficiency about 40% increased as a result of doubling the membrane length.

5. Commemoration

The authors are particularly grateful to Prof. Mohammad Khoshnoodi from University of Sistan and Baluchestan, the project manager who passed away unexpectedly, for his suggestions and knowledge shared.

REFERENCES

- [1] R. Faiz and M. Al-Marzouqi, “Mathematical Modeling for the Simultaneous Absorption of CO₂ and H₂S Using MEA in Hollow Fiber Membrane Contactors,” *Journal of Membrane Science*, Vol. 342, No. 1-2, 2009, pp. 269-278. doi:10.1016/j.memsci.2009.06.050
- [2] R. N. Maddox, “Gas Conditioning and Processing,” *Cam-*

- pbell Petroleum Series*, 3rd Edition, Vol. 4, 1982.
- [3] L. Sumin, *et al.*, "The Enhancement of CO₂ Chemical Absorption by K₂CO₃ Aqueous Solution in the Presence of Activated Carbon Particles," *Chinese Journal of Chemical Engineering*, Vol. 15, No. 6, 2007, pp. 842-846. doi:10.1016/S1004-9541(08)60012-9
- [4] A. Mandowara and P. K. Bhattacharya, "Membrane Contactor as Degasser Operated under Vacuum for Ammonia Removal from Water: A Numerical Simulation of Mass Transfer under Laminar Flow Conditions," *Computers and Chemical Engineering*, Vol. 33, No. 6, 2009, pp. 1123-1131. doi:10.1016/j.compchemeng.2008.12.005
- [5] A. Gabelman and S. T. Hwang, "Hollow Fiber Membrane Contactors," *Journal of Membrane Science*, Vol. 159, No. 1-2, 1999, pp. 61-106. doi:10.1016/S0376-7388(99)00040-X
- [6] V. Y. Dindore, D. W. F. Brilman and G. F. Versteeg, "Modelling of Cross-Flow Membrane Contactors: Mass Transfer with Chemical Reactions," *Journal of Membrane Science*, Vol. 225, No. 1-2, 2005, pp. 275-289. doi:10.1016/j.memsci.2005.01.042
- [7] H. Jeon, *et al.*, "Absorption of Sulfur Dioxide by Porous Hydrophobic Membrane Contactor," *Desalination*, Vol. 234, No. 1-3, 2008, pp. 252-260. doi:10.1016/j.desal.2007.09.092
- [8] K. A. Hoff, *et al.*, "Modeling and Experimental Study of Carbon Dioxide Absorption in Aqueous Alkanolamine Solutions Using a Membrane Contactor," *Industrial & Engineering Chemistry Research*, Vol. 43, No. 16, 2004, pp. 4908-4921. doi:10.1021/ie034325a
- [9] A. Kohl and R. Nielsen, "Gas Purification," 5th Edition, Gulf Publishing Company, Houston, 1997.
- [10] G. Hochgesand, "Rectisol and Purisol," *European and Japanese Chemical Industrials Symposium*, 1970, Vol. 62, No. 7, pp. 37-43.
- [11] J. A. Delgado, *et al.*, "Simulation of CO₂ Absorption into Aqueous DEA Using a Hollow Fiber Membrane Contactor: Evaluation of Contactor Performance," *Chemical Engineering Journal*, Vol. 62, 2009, pp. 396-405. doi:10.1016/j.cej.2009.04.064
- [12] R. Wang, D. F. Li and D. T. Liang, "Modeling of CO₂ Capture by Three Typical Amine Solutions in Hollow Fiber Membrane Contactors," *Chemical Engineering and Processing*, Vol. 43, No. 7, 2004, pp. 849-856. doi:10.1016/S0255-2701(03)00105-3
- [13] W. Rongwong, R. Jiratananon and S. Atchariyawut, "Experimental Study on Membrane Wetting In Gas-Liquid Membrane Contacting Process for CO₂ Absorption by Single and Mixed Absorbents," *Separation and Purification Technology*, Vol. 69, 2009, pp. 118-125. doi:10.1016/j.seppur.2009.07.009
- [14] D. Wang, W. K. Teo and K. Li, "Removal of H₂S to Ultra-Low Concentrations Using an Asymmetric Hollow Fibre Membrane Module," *Separation and Purification Technology*, Vol. 27, No. 1, 2002, pp. 33-40. doi:10.1016/S1383-5866(01)00186-1
- [15] P. Keshavarz, J. Fathhikalajahi and S. Ayatollahi, "Mathematical Modeling of the Simultaneous Absorption of Carbon Dioxide and Hydrogen Sulfide in a Hollow Fiber Membrane Contactor," *Separation and Purification Technology*, Vol. 63, No. 1, 2008, pp. 145-155. doi:10.1016/j.seppur.2008.04.008
- [16] S. Wang, K. Hawboldt and M. A. Abdi, "Novel Dual-Membrane Gas-Liquid Contactors: Modelling and Concept Analysis," *Industrial & Engineering Chemistry Research*, Vol. 45, No. 23, 2006, pp. 7882-7891. doi:10.1021/ie051368d
- [17] A. Mansourizadeh, A. F. Ismail and T. Matsuura, "Effect of Operating Conditions on the Physical and Chemical CO₂ Absorption through the PVDF Hollow Fiber Membrane Contactor," *Journal of Membrane Science*, Vol. 353, No. 1-2, 2010, pp. 192-200. doi:10.1016/j.memsci.2010.02.054
- [18] R. Faiz and M. Al-Marzouqi, "CO₂ Removal from Natural Gas at High Pressure Using Membrane Contactors: Model Validation and Membrane Parametric Studies," *Journal of Membrane Science*, Vol. 365, No. 1-2, 2010, pp. 232-241. doi:10.1016/j.memsci.2010.09.004
- [19] J. Happel, "Viscous Flow relative to Arrays of Cylinders," *AIChE Journal*, Vol. 5, No. 2, 1959, pp. 174-177. doi:10.1002/aic.690050211
- [20] M. Al-Marzouqi, *et al.*, "Modeling of CO₂ Absorption in Membrane Contactors," *Separation and Purification Technology*, Vol. 59, No. 1, 2008, pp. 286-293.
- [21] M. Mavroudi, S. P. Kaldis and G. P. Sakellariopoulos, "Reduction of CO₂ Emissions by a Membrane Contacting Process," *Fuel*, Vol. 82, No. 15-17, 2003, pp. 2153-2159. doi:10.1016/S0016-2361(03)00154-6
- [22] P. Keshavarz, J. Fathhikalajahi and S. Ayatollahi, "Analysis of CO₂ Separation and Simulation of a Partially Wet-Ted Hollow Fiber Membrane Contactor," *Journal of Hazardous Materials*, Vol. 152, No. 3, 2008, pp. 1237-1247. doi:10.1016/j.jhazmat.2007.07.115
- [23] G. F. Versteeg and W. P. M. Van Swaaij, "On the Kinetics between CO₂ and Alkanolamines both in Aqueous and Non-Aqueous Solutions I. Primary and Secondary Amines," *Chemical Engineering Science*, Vol. 43, No. 3, 1988, pp. 573-585. doi:10.1016/0009-2509(88)87017-9
- [24] J. J. Carroll and A. E. Mather, "The Solubility of Hydrogen Sulphide in Water from 0°C to 90°C and Pressure to 1 MPa," *Geochimica et Cosmochimica Acta*, Vol. 53, No. 6, 1989, pp. 1163-1170. doi:10.1016/0016-7037(89)90053-7
- [25] K. Lunsford and G. McIntyre, "Decreasing Contactor Temperature Could Increase Performance," *GPA Annual Convention*, Bryan Research and Engineering, Inc., Texas, 1999, pp. 121-127.
- [26] E. L. Cussler, "Diffusion Mass Transfer in Fluid Systems," Cambridge University, Cambridge, 1984.
- [27] M. V. Diaz and A. Coca J., "Correlation for the Estimation of Gas-Liquid Diffusivity," *Chemical Engineering Communications*, Vol. 52, No. 4-6, 1987, pp. 271-281. doi:10.1080/00986448708911872
- [28] R. H. Perry, "Perry's Chemical Engineers' Handbook," 7th Edition, McGraw-Hill, New York, 1997.
- [29] B. E. Poling, J. M. Prausnitz and J. P. O'Connell, "The

- Properties of Gases and Liquids,” 5th Edition, McGraw-Hill, New York, 2004.
- [30] R. Faiz and M. Al-Marzouqi, “H₂S Absorption via Carbonate Solution in Membrane Contactors: Effect of Species,” *Journal of Membrane Science*, Vol. 350, No. 1-2, 2010, pp. 200-210. [doi:10.1016/j.memsci.2009.12.028](https://doi.org/10.1016/j.memsci.2009.12.028)
- [31] V. Y. Dindore, D. W. F. Brilman and G. F. Versteeg, “Hollow Fiber Membrane Contactor as a Gas-Liquid Model Contactor,” *Chemical Engineering Science*, Vol. 60, No. 2, 2005, pp. 467-479. [doi:10.1016/j.ces.2004.07.129](https://doi.org/10.1016/j.ces.2004.07.129)

Nomenclature

| | |
|-------------------------|---|
| C | Concentration, mol/m ³ |
| C_0 | Initial concentration, mol/m ³ |
| $C_{i\text{-phase}}$ | Concentration of any component in the gas or membrane or liquid phase, mol/m ³ |
| $C_{0, i\text{-phase}}$ | Initial concentration of any component in the gas or liquid phase, mol/m ³ |
| D | Diffusion coefficient, m ² /s |
| $D_{i\text{-phase}}$ | Diffusion coefficient of any gas in the gas or membrane or liquid phase, m ² /s |
| L | Filer length, m |
| m_i | Distribution coefficient of component i in the absorbent solvent, liquid mol/gas mol |
| n | Number of fiber in module |
| r | Radial coordinate, m |
| r_1 | Inner tube radius, m |
| r_2 | Outer tube radius, m |
| r_3 | Happel’s free surface model radius, m |
| r_4 | Inner module radius, m |
| R | Reaction rate, mol/m ³ s |
| $R_{i\text{-phase}}$ | Reaction rate of component i in the gas or membrane or liquid phase, mol·m ⁻³ ·s ⁻¹ |
| V | Axial velocity, m/s |
| $V_{i\text{-phase}}$ | Axial velocity of component i in the tube or shell sides, m/s |
| V_{shell} | Axial velocity component in the shell, m/s |
| $V_{\text{avg-shell}}$ | Average axial velocity component in the shell, m/s |
| V_{tube} | Axial velocity component in the tube, m/s |
| $V_{\text{avg-tube}}$ | Average axial velocity component in the tube, m/s |
| z | Axial coordinate, m |
| ε | Membrane porosity |
| τ | Membrane tortuosity |
| ϕ | Volume fraction of the void inside the membrane gas absorber module |

Subscripts

| | |
|---------|--|
| i | CO ₂ or H ₂ S present in the gas or membrane or liquid phase |
| mem | Membrane phase within the model domain |
| dry mem | Non wetted part of membrane phase within the model domain |
| wet mem | Wetted part of membrane phase within the model domain |
| shell | Shell phase within the model domain |
| solvent | Absorbent solvent |
| shell | Shell phase within the model domain |
